JOC The Journal of Organic Chemistry

Article

pubs.acs.org/joc

Symmetrical Imidazolium Chloride Based on (−)-Menthol: Synthesis, Characterization, and Theoretical Model of the Reaction

Joanna Feder-Kubis,*[,†] Borys Szefczyk,[†] and Maciej Kubicki[‡]

[†]Wrocław University of Technology, Faculty of Chemistry, Wybrzeże Wyspiańskiego 27, 50-370 Wrocław, Poland

[‡]Adam Mickiewicz University in Poznań, Faculty of Chemistry, Umultowska 89b, 61-614 Poznań, Poland

Supporting Information

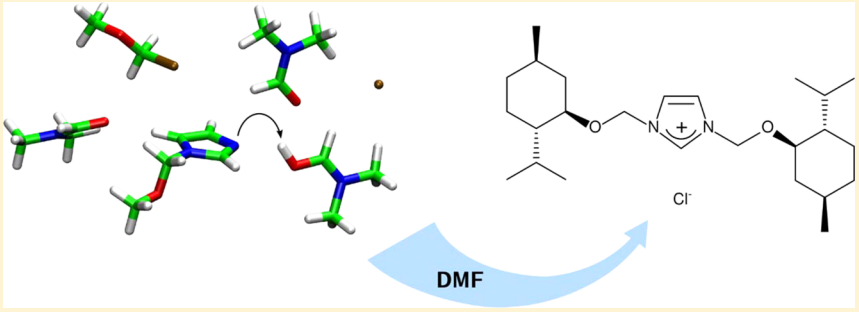

ABSTRACT: New symmetrical imidazolium chloride from a natural chiral pool of (1*R*,2*S*,5*R*)-(−)-menthol can be efficiently prepared by two different methods. The first method involves a specific type of Menschutkin reaction using novel 1-(1*R*,2*S*,5*R*)-(−)-menthoxymethylimidazole as amine, chloromethyl (1*R*,2*S*,5*R*)-(−)-menthyl ether as quaternization agent, and hexane as solvent. In the second method, imidazole, chloromethyl (1*R*,2*S*,5*R*)-(−)-menthyl ether, and DMF are used. To understand this specific type of the reaction, quantum chemical calculations at the DFT level have been used. The preparation and characterization of 1,3-bis[(1*R*,2*S*,5*R*)-(−)-menthoxymethyl]imidazolium chloride are reported.

INTRODUCTION

One of the most rapidly growing areas of chemistry research involves ionic liquids (ILs). The asymmetrical nature of the cation plays a major role in explanation why certain salts have such low melting points.[1−5] However, even symmetrical ILs were found to be liquids.[6,7] In particular, Dzyba and Bartsch reported that 1,3-dialkylimidazolium salt hexafluorophosphates with dibutyl, dipentyl, dioctyl, dinonyl, and dodecyl substituents were found to be RTILs.[8] For long enough alkyl chain lengths, symmetrical substituted 1,3-dialkylimidazolium salts exhibit liquid crystalline properties.[9]

The majority of symmetric ILs (primarily when symmetry is due to the presence of two identical chains in a cation, but also in the case of dicationic and tricationic ILs) have been shown to possess superior physical properties in terms of thermal stability and volatility compared to traditional ionic liquids (ILs).[10−14] Zheng et al. described an effect of cation symmetry on the morphology and physicochemical properties of imidazolium ionic liquids.[11] 1,3-Dialkylimidazolium bis(trifluoromethylsulfonyl)imide ($[(C_{N/2})_2im][NTf_2]$) has been compared to 1-alkyl-3-methylimidazolium bis(trifluoromethylsulfonyl)imide ($[C_{N\text{-}1}C_1im][NTf_2]$) for N = 4, 6, 8, and 10. For the given pair of ionic liquids with the same N, the ILs differ only in the symmetry of the alkyl substitution in the imidazolium ring of the cation. Small-wide-angle X-ray scattering measurements indicate that the structural heterogeneities are larger in the asymmetric IL than in the symmetric IL. Symmetric ILs with N = 4 and 6 easily crystallize, whereas longer alkyl chains and asymmetry hinder crystallization. Extremely interesting is the fact that the glass transition temperature is found to vary inversely with the correlation length of structural heterogeneities and with the length of the longest alkyl chain. Whereas the densities for a symmetric/asymmetric IL pair with a given N are nearly the same, the viscosity of the asymmetric IL is greater than that of the symmetric IL. Likewise, the effect of symmetry on the physical properties of variety of dicationic ionic liquids has been explored.[15] The symmetrical cationic ILs in the studied group generally tend to have higher densities than their unsymmetrical analogues. It has been also shown that dicationic ILs show much higher thermal stabilities than monocationic ILs.

Consequently, they have been proposed as novel high-temperature lubricants,[16] solvents in high-temperature reactions,[17−19] ultrastable separation phases,[20,21] and in mass spectrometry where ordinary ILs fail.[22,23] Furthermore, biological properties of symmetrical ILs should not be overlooked, such as their tribological properties as ultrathin films[24] and promising results in the area of microbiology.[25]

We have already described asymmetrical ionic liquids obtained directly from the natural chiral pool of (1*R*,2*S*,5*R*)-(−)-menthol.[26−29] Herein we report the synthesis and

Received: October 9, 2014
Published: December 1, 2014

Scheme 1. Synthesis of 1-(1*R*,2*S*,5*R*)-(−)-Menthoxymethylimidazole

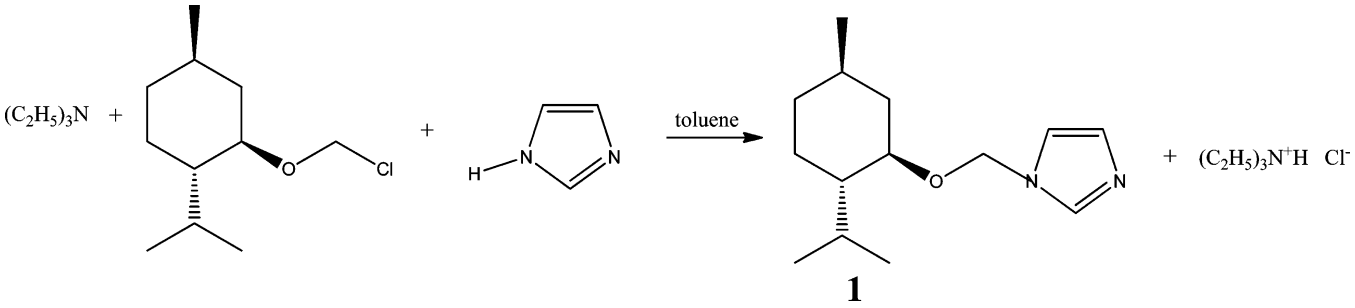

properties of symmetrical imidazolium chloride with two (1*R*,2*S*,5*R*)-(−)-menthoxymethyl substituents.

RESULTS AND DISCUSSION

1. Synthesis, Properties, and Structure of 1-(1*R*,2*S*,5*R*)-(−)-Menthoxymethylimidazole. *1.1. Synthesis and Properties of 1-(1R,2S,5R)-(−)-Menthoxymethylimidazole.* In order to obtain 1,3-bis[(1*R*,2*S*,5*R*)-(−)-menthoxymethyl]imidazolium chloride first the 1-(1*R*,2*S*,5*R*)-(−)-menthoxymethylimidazole (**1**) was prepared in toluene, according to the summary given in Scheme 1. In the first step, triethylamine was reacted with the freshly distilled chloromethyl (1*R*,2*S*,5*R*)-(−)-menthyl ether to give triethyl-[(1*R*,2*S*,5*R*)-(−)-menthoxymethyl]ammonium chloride. Chloromethyl (1*R*,2*S*,5*R*)-(−)-menthyl ether was obtained by chloromethylation of (1*R*,2*S*,5*R*)-(−)-menthol.[26] This ether is an excellent reagent, but it is readily hydrolyzed to HCl, CH_2O, and menthol. These reactions should therefore be conducted under strictly anhydrous conditions. The second step consisted of the *N*-alkoxymethylation of the imidazole with the triethyl[(1*R*,2*S*,5*R*)-(−)-menthoxymethyl]ammonium chloride.

The crude product was distilled from the reaction mixture (177 °C @ 0.75 mmHg). After the product was cooled to room temperature, solidification of the pure, colorless liquids was observed. Finally, the solid 1-(1*R*,2*S*,5*R*)-(−)-menthoxymethylimidazole was obtained with 91% yield. The new chiral imidazole derivative crystallized easily from hexane−acetone to form long needles with a sharp and low melting point 48−50 °C (with 98% yield of crystallization). The specific rotation of new 1-(1*R*,2*S*,5*R*)-(−)-menthoxymethylimidazole (**1**) measured in ethanol is $[\alpha]^{20}_{D} = -132.1$ (*c* 0.8). The compound **1** is miscible at room temperature with low molecular weight alcohols, acetone, ethyl acetate, chloroform, DMF, THF, toluene, hexane, and diethyl ether but immiscible in water.

1.2. X-ray Structure of 1-(1R,2S,5R)-(−)-Menthoxymethylimidazole. In order to confirm the reaction path, X-ray structure analysis of the product was performed. Because of the low melting point and the relatively poor diffraction, the low temperature data collection was deemed necessary. Figure 1 shows that, in fact, compound **1** was obtained. The molecular dimensions are typical; the oxomethylimidazole substituent occupies the equatorial position and the orientation of imidazole ring can be described by the COCN torsion angle of −70.9(2)° (that means that the COC bridge is almost perpendicular to the imidazole ring plane). Such a folded conformation might be additionally stabilized by the H1···N13 intramolecular interactions. In the crystal structure weak intermolecular C5−H5···O11, C14−H14···N12, and C−H···π (C11−H11B···C_g(imidazole)) hydrogen bond-type contacts

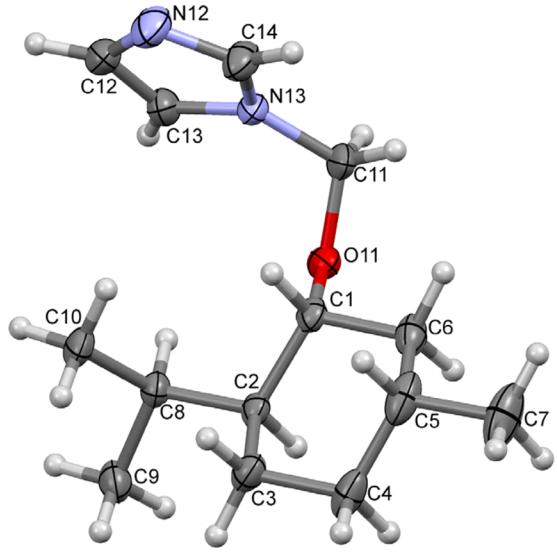

Figure 1. Perspective view of the molecule **1** with numbering scheme. The ellipsoids are drawn at 50% probability level; hydrogen atoms are shown as spheres of arbitrary radii.

connect molecules into a three-dimensional structure (details in Table S1 and Figure S1, Supporting Information).

2. Synthesis, Properties, Theoretical Model, and Structure of 1,3-Bis[(1*R*,2*S*,5*R*)-(−)-menthoxymethyl]-imidazolium Chloride. *2.1. Synthesis and Properties of 1,3-Bis[(1R,2S,5R)-(−)-menthoxymethyl]imidazolium Chloride.* 1,3-Bis[(1*R*,2*S*,5*R*)-(−)-menthoxymethyl]imidazolium chloride was obtained by two methods.

In the first method the symmetrical chiral imidazolium chloride was prepared by Menschutkin reaction. Quaternization was achieved using the 1-(1*R*,2*S*,5*R*)-(−)-menthoxymethylimidazole and freshly distilled chloromethyl (1*R*,2*S*,5*R*)-(−)-menthyl ether. As mentioned earlier, this ether is very reactive and, therefore, requires strictly anhydrous conditions because otherwise it readily becomes hydrolyzed to HCl, CH_2O, and menthol. Anhydrous hexane proved to be a suitable solvent in this case, and the product precipitated from such solution. Quaternization takes place immediately and proceeds readily at room temperature.

The exact synthesis of 1,3-bis[(1*R*,2*S*,5*R*)-(−)-menthoxymethyl]imidazolium chloride (**2**), which has been prepared by this procedure, is presented in Scheme 2. In general, the procedure is simple and the reaction has high product yield (93%).

In the second method 1,3-bis[(1*R*,2*S*,5*R*)-(−)-menthoxymethyl]imidazolium chloride (**2**) was obtained using imidazole

dx.doi.org/10.1021/jo502317m | J. Org. Chem. 2015, 80, 237−246

Scheme 2. Synthesis of 1,3-Bis[(1*R*,2*S*,5*R*)-(−)-menthoxymethyl]imidazolium Chloride from 1-(1*R*,2*S*,5*R*)-(−)-Menthoxymethylimidazole (Method I)

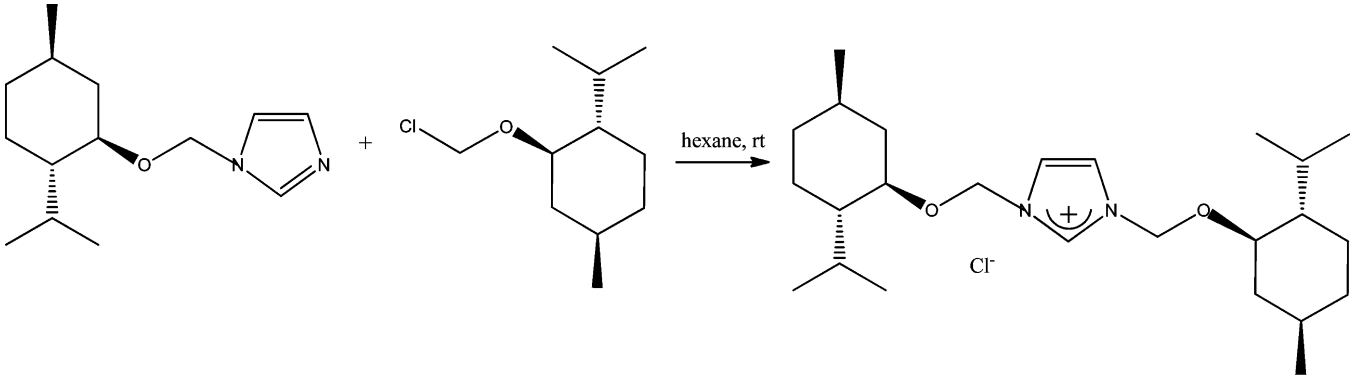

1 **2**

Scheme 3. Synthesis of 1,3-Bis[(1*R*,2*S*,5*R*)-(−)-menthoxymethyl]imidazolium Chloride from Imidazole (Method II)

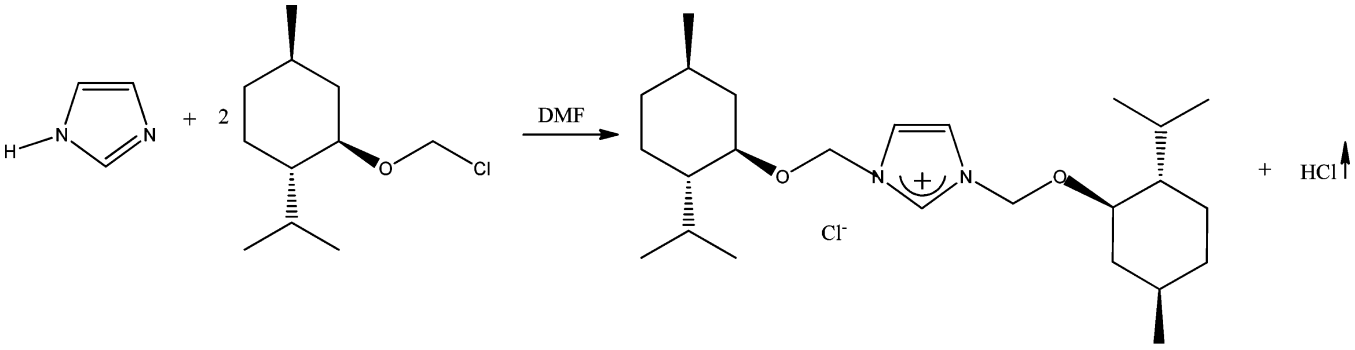

2

and chloromethyl (1*R*,2*S*,5*R*)-(−)-menthyl ether as reactants and DMF as a solvent (Scheme 3).

The type of solvent employed was found to play a significant role in determining the course of the reaction: only in anhydrous DMF was a single product **2** obtained. The reaction took place in the absence of alkali, and the total efficiency of the process reached 83.5%. When the process was attempted in any other anhydrous solvent, such as acetone, toluene, or DMSO, the reaction product contained three salts: **2**, $\mathbf{1}^+$ hydrochloride, and imidazolium hydrochloride, the separation of which was practically impossible. The one-step approach for the synthesis of symmetrical chiral imidazolium chloride, using anhydrous DMF, described herein proved to be very effective.

A similar reaction has been already described for 1,3-dialkoxymethylimidazolium chlorides,[30] but no mechanistic model has been proposed. Here, in section 2.2, we present the theoretical model of the synthesis of 1,3-bis[(1*R*,2*S*,5*R*)-(−)-menthoxymethyl]imidazolium chloride using DMF as a solvent.

Obtained in those two different procedures, 1,3-bis-[(1*R*,2*S*,5*R*)-(−)-menthoxymethyl]imidazolium chloride **2** was crystallized from ethyl acetate to form white plates with a sharp melting point: 126−127.7 °C. Unfortunately, despite many trials, no crystals suitable for X-ray diffraction experiments were obtained. The specific rotation of compound **2** measured in ethanol is $[\alpha]^{20}_{D}$= −130.8 (*c* 0.9). The purity of this new chiral chloride was determined by a direct two-phase titration technique (EN ISO 2871-2:2010) using menthol as solvent and achieved 99.3% for crystallized chloride. 1,3-Bis-[(1*R*,2*S*,5*R*)-(−)-menthoxymethyl]imidazolium chloride is soluble at room temperature in methanol, ethanol, 1-propanol, 2-propanol, DMF, THF, toluene, and chloroform, but not in hexane, diethyl ether, and water. At elevated temperatures the chloride **2** has been found to dissolve also in acetone, and ethyl acetate.

There are notable differences between the two methods of synthesis. The one-step method (method II) clearly simplifies and accelerates the process; however, it has its drawbacks. The product (**2**) is dissolved in the reaction medium, so it is necessary to evaporate the solvent under reduced pressure. The crude product was obtained as light yellow solid with a tendency to oil, which greatly complicates the process of purification and crystallization. On the other hand synthesis according to method I, from 1-(1*R*,2*S*,5*R*)-(−)-menthoxymethylimidazole, leads to a snow-white product whose purification and crystallization does not pose any problems. The purity of crude chiral chloride, determined by a direct two-phase titration technique (EN ISO 2871-2:2010), using menthol as solvent achieved 97.1% for method II, while 98.8% for method I. Moreover, the yield of the two-step reaction (method I) is 93% and of one-step reaction (method II) is 83.5%.

Additionally, there is the interesting subject of the effect of symmetry on melting points. Previously, we have synthesized asymmetrical 3-(alkoxymethyl)-1-(1*R*,2*S*,5*R*)-(−)-(menthoxymethyl)imidazolium chlorides (from ethoxymethyl to dodecyloxymethyl).[29] Only 3-(ethoxymethyl)-1-(1*R*,2*S*,5*R*)-(−)-(menthoxymethyl)imidazolium chloride is solid with a melting temperature 55−58 °C; all other chlorides from this

dx.doi.org/10.1021/jo502317m | *J. Org. Chem.* 2015, 80, 237−246

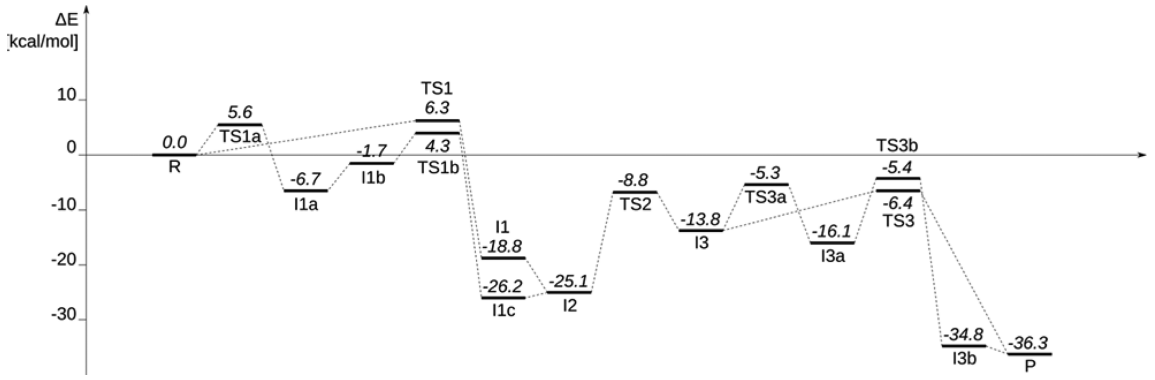

Figure 2. Overall energy profile of the reaction.

homologous series are oils, while presented here the symmetrical 1,3-bis[(1*R*,2*S*,5*R*)-(−)-menthoxymethyl]imidazolium chloride has a much higher melting temperature (126−127.7 °C, method I). Therefore, the asymmetry of the cation seems to be an important factor in lowering the melting points.[1−5,31]

2.2. Theoretical Model of the Synthesis of 1,3-Bis-[(1R,2S,5R)-(−)-menthoxymethyl]imidazolium Chloride. The aim of the quantum chemical calculations (cf. Experimental Section for the approximations used) was to verify the following hypothesis: the reaction used in the one-step synthesis of the symmetrical salt (section 2.1) proceeds in three consecutive steps. Step 1 (from R to I2) is a substitution of chloromethyl ether (to N3 atom of imidazole). The resulting product is a monosubstituted imidazolium salt, which has to undergo deprotonation (step 2, from I2 to I3), before it can be substituted at the second nitrogen atom. After deprotonation, the intermediate undergoes a second substitution to N1 atom of the imidazole ring (step 3, from I3 to P). These three steps and corresponding systems are shown in Figures 2−5 and Table 1. This hypothesis has been proven to be plausible, and moreover, it seems that only in DMF can a direct deprotonation of the first 3*N*-methoxymethylimidazole be performed. This is because the DMF dimer is able to stabilize H^+, which renders it distinct from other solvents used.

Table 1. Energy of the Minima and Saddle Points along the Reaction Path (kcal/mol)

step	Δ*E* (X3LYP)	Δ*E* (MP2//X3LYP)	Δ*G* (X3LYP)
R	0.0	0.0	0.0
TS1	6.3	9.1	8.1
TS1a	5.6	5.2	10.7
I1a	−6.7	−9.1	2.1
I1b	−1.7	−2.3	4.1
TS1b	4.3	5.8	8.8
I1	−18.8	−18.6	−11.3
I1c	−26.2	−27.8	−18.3
I2	−25.1	−26.1	−15.8
TS2	−8.8	−10.3	1.0
I3	−13.8	−11.8	−7.3
TS3	−6.4	1.8	1.4
TS3a	−5.3	1.0	5.5
I3a	−16.1	−14.3	−3.8
TS3b	−5.4	0.0	5.4
I3b	−34.8	−33.1	−21.6
P	−36.3	−35.3	−22.2

Step 1, First Substitution at N3. The nucleophilic substitution of chloromethyl ether to N3 atom of imidazole can proceed via S_N2 mechanism. The barrier for the substitution of chloromethyl ether directly to N3, calculated at X3LYP level of theory, is 6.3 kcal/mol. The Gibbs free energy of activation, computed as described in the Experimental section, is 8.1 kcal/mol. The energy of activation corrected at the MP2 level of theory is 9.1 kcal/mol. This step is exoergic, and the X3LYP reaction energy is −25.1 kcal/mol. However, the first step of the reaction can take an alternative route. Namely, the chloromethyl ether can be transferred to DMF molecule (through TS1a; X3LYP barrier is 6.0 kcal/mol, MP2//X3LYP barrier is 8.1 kcal/mol and X3LYP Δ*G* is 12.9 kcal/mol) and after passing two intermediates (I1a, I1b) it can be transferred to imidazole (through TS1b; X3LYP barrier is 4.3, MP2//X3LYP is 5.8 and X3LYP Δ*G* is 8.8 kcal/mol). The barriers for the two alternative routes are comparable, yet one has to remember that there is abundance of DMF compared to imidazole; therefore, the second route seems more likely. Moreover, TS1a and TS1b at the molecular level are passed through the S_N2 mechanism (see Figures 3 and 5). There is a chemical bond formed between chloromethyl ether and the solvent molecule; therefore, it might be treated as two consecutive S_N2 reactions. Nevertheless, the whole step might be considered an S_N1 reaction with chloromethyl ether cation stabilized by DMF molecule, and experimentally, it would be observed as an S_N1 reaction since there is inversion of configuration. Figure 3 shows the two alternative routes: in the upper row, reaction proceeds through direct transfer to imidazole (S_N2 mechanism), while in the bottom row, intermediates I1a and I1b feature a carbocation stabilized by DMF (S_N1-like mechanism). The structures of the reactant, transition state, and intermediate complexes are shown in Figure 5, and the coordinates are deposited as the Supporting Information. The first step was also used to verify how the different environment models influence the energy barrier; namely, the step was recalculated with no solvent and then with one and two DMF molecules that do not take part directly in the reaction at this stage. It has been also recalculated using implicit solvent, represented by the PCM model. As shown in Table 2, the barrier for the substitution in vacuum is 29 kcal/mol. It can be reduced to ca. 17 kcal/mol, when two explicit solvent molecules are taken into account. It can be further reduced to 9 kcal/mol if the long-range effects of the solvent are included as well (by means of the PCM model). In principle, the main part of the barrier reduction is contributed by the PCM model, since for the Ini-0/PCM (no DMF

dx.doi.org/10.1021/jo502317m | J. Org. Chem. 2015, 80, 237−246

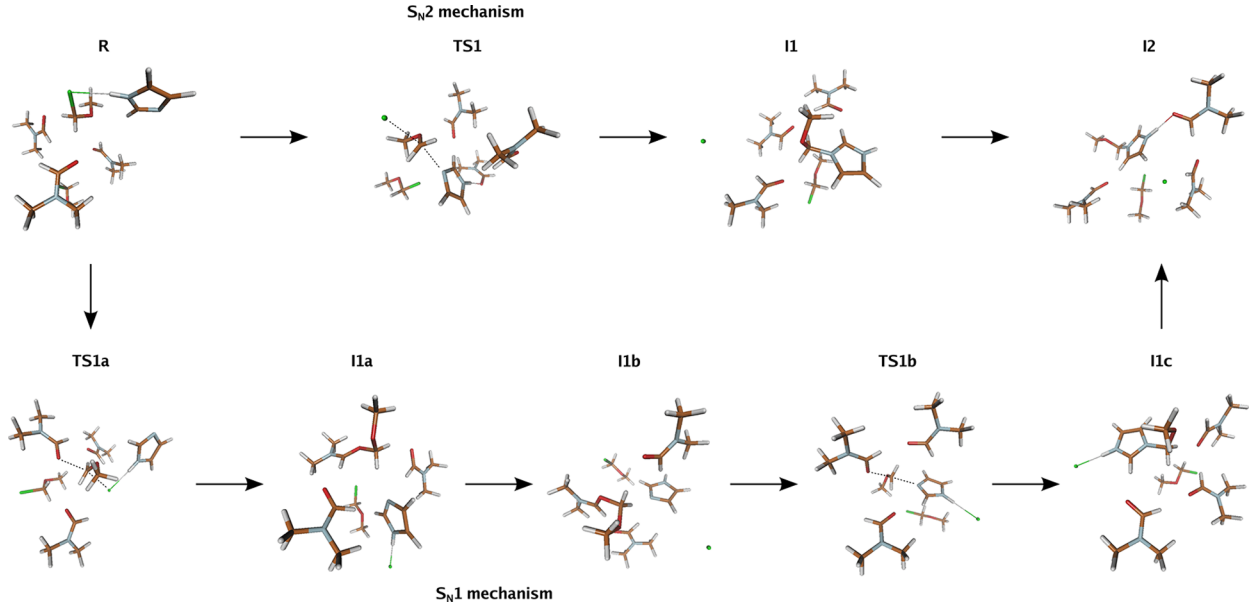

Figure 3. Alternative mechanisms of the step 1 (going from R to I2). Upper row corresponds to direct transfer to imidazole, while in the bottom row, the transfer is mediated by DMF molecule.

Table 2. Effect of the Environment on the Activation Barrier Height and Reaction Energy: Implicit and Explicit Solvent. Energies in (kcal/mol), calculated using DFT (X3LYP)

		Δ*E*			Δ*G*		
	model	R1	TS1	I1	R1	TS1	I1
vacuum	Ini-0	0.0	29.0	3.3	0.0	31.2	7.2
1DMF	Ini-1	0.0	24.2	−9.4	0.0	25.4	−3.7
2 DMF	Ini-2	0.0	16.8	−7.4	0.0	20.3	−2.8
PCM	Ini-0/ PCM	0.0	9.7	−18.5	0.0	12.5	−12.7
1DMF + PCM	Ini-1/ PCM	0.0	9.3	−22.1	0.0	12.1	−15.4
2DMF + PCM	Ini-2/ PCM	0.0	9.0	−18.1	0.0	16.3	−11.7

molecules, but PCM included) the barrier is 9.7 kcal/mol. Based on that, we have decided to use the PCM model in our calculations and also to include three explicit DMF because they directly take part in the substitution reactions and proton trapping; they also stabilize the chloromethyl cation. Therefore, all of the results regarding steps 1−3 of the reaction are based on calculations with explicit (three DMF molecules) and inexplicit (PCM) solvent. As Table 1 shows, adding the third DMF molecule reduces the barrier even more (to 6.3 kcal/mol at X3LYP level, Δ*G* equals to 8.1 kcal/mol). Adding more solvent molecules could reduce the barrier further, but it would be impractical for computational reasons (increase of CPU time, number of degrees of freedom and number of local minima). The direct transfer of chloromethyl ether proceeds through a slightly asymmetric transition state (TS1, Figures 3 and 5); i.e., the CL−C1−O and O−C1−N3 angles are not right and amount to 104 and 100°, respectively. The CL−C1 distance is 2.51 Å, and the C1−N3 distance is 2.37 Å. The reaction is accompanied by charge redistribution necessary to form the cation−anion pair (Table 4): the negative charge at N3 (−0.70e) is reduced to −0.39e in the TS and then to +0.06e in the I1. The chlorine atom in the chloromethyl ether has charge −0.22/-0.30e (depending on which molecule is considered) and decreases to −0.97e in I1. As a result, the

Table 3. Proton Transfer from Substituted Intermediate I1 to a Free Imidazole Molecule. Energies in (kcal/mol), calculated using DFT (X3LYP)

	Δ*E*	Δ*G*
Ri	0.0	0.0
TSi	2.5	0.6
Ii	−0.9	−1.1

C1−O bond in the ether becomes more polarized at the TS1 (−0.63e at C1 and −0.30e at O) and at the I1 (0.43e at C1 and −0.50e at O. The chloromethyl ether transfer mediated by DMF proceeds through TS1a transition state, which is also slightly bent (angles CL−C1−O and O−C1−N3 equal to 103 and 102°, respectively). The CL−C1 distance is slightly longer (2.73 Å) and the C1−O distance is shorter than C1−N3 in TS1 (2.26 Å). Subsequently, the system passes through TS1b, which is also bent (angles equal to 99 and 102°), but with very symmetric bond lengths (2.31 and 2.33 Å for O−C1 and C1−N3, respectively). It seems that the TS1a (transfer of chloromethyl ether to DMF) has an electronic structure similar to TS1, since the charges at the CL, C1, and O atoms of the chloromethyl ether are quite similar (Table 4).

Deprotonation of the Intermediate. The deprotonation of the first intermediate can proceed in an almost barrierless manner to another unsubstituted imidazole (Table 3); however, this does not explain the different mechanism in DMF than in other solvents.

Conversely, it seems possible only in DMF that the solvent is directly involved in the process and catalyzes the deprotonation. Namely, a dimer of DMF molecules is able to cleave the N1−H bond and stabilize the dissociated H^+, Cl^- pair. This is because the imide moiety of DMF has partially aromatic character (it is also planar) and is a good proton acceptor.[32] The postulated ability to stabilize the dissociated H^+, Cl^- pair—and specifically by a DMF pair instead of a single molecule—has been confirmed in spectroscopic experiments.[33,34] The barrier for the proton transfer is slightly high (around 16 kcal/mol, regardless of the level of theory, Table 1);

dx.doi.org/10.1021/jo502317m | J. Org. Chem. 2015, 80, 237−246

Table 4. CHELPG Charges at Selected Centers of the Species Involved into the First Step of the Reaction. Charges Computed at X3LYP/6-31+G(d)//MP2/6-31+G(d) Level of Theory

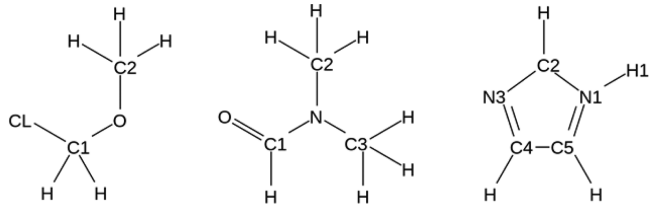

	imidazole						ether			DMF		
	N1	H1	C2H[a]	N3	C4H[a]	C5H[a]	CL	C1H$_2$[a]	O	O	C1H[a]	N
R	−0.240	0.334	0.373	−0.702	0.275	−0.075	−0.303	0.324	−0.185	−0.595	0.437	−0.101
							−0.219[b]	0.404[b]	−0.444[b]	−0.651[b]	0.479[b]	−0.074[b]
										−0.675[b]	0.480[b]	−0.103[b]
TS1	−0.063	0.279	0.316	−0.395	0.089	−0.032	−0.825	0.635	−0.298			
I2	−0.182	0.383	0.211	0.060	−0.124	−0.056	−0.975	0.430	−0.499			
TS1a	−0.200	0.328	0.375	−0.720	0.280	−0.107	−0.842	0.639	−0.269	−0.563	0.478	0.127
I1a	−0.185	0.346	0.151	−0.245	0.098	−0.043	−0.941	0.587	−0.501	−0.423	0.483	0.046
I1b	−0.137	0.326	0.112	−0.259	0.167	−0.061	−0.977	0.538	−0.473	−0.405	0.487	−0.001
TS1b	−0.115	0.316	0.077	−0.181	0.028	0.064	−0.931	0.533	−0.365	−0.423	0.367	−0.031
I1c	−0.286	0.419	0.212	0.207	−0.011	0.162	−0.917	0.348	−0.455	−0.467	0.328	−0.040
										−0.509[b]	0.403[b]	−0.090[b]
										−0.572[b]	0.425[b]	−0.103[b]

[a]Hydrogen atom charges added to heavy atom. [b]Charges on second/third DMF molecule.

however, the energy of the resulting transition state complex TS2 is still ca. −9 kcal/mol below the initial reactant complex R. Also, the height of the barrier for the proton transfer is possibly further decreased by tunneling, which is not taken into account in our calculations. The proton transfer from the intermediate to the DMF pair has a quite complex nature: there are three molecules participating—the substituted imidazole and two solvent molecules. Despite many trials, we did not succeed in finding the corresponding transition state for a proton transfer to a single DMF molecule. Moreover, the path of the proton transfer seems to be quite complex as well. Figure 4 shows an IRC profile: the proton is first transferred to one of the DMF molecules, and only then is it captured by the oxygen of the other DMF molecule and trapped between the two solvent molecules. This results in a profile with an apparent kink (see the inset in Figure 4). In fact, the slope of the curve

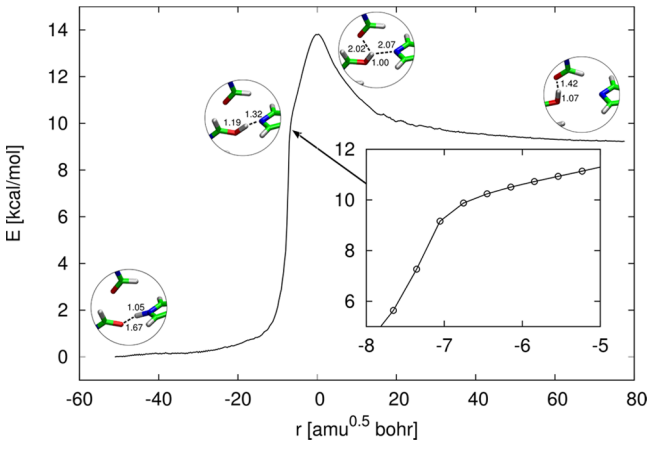

Figure 4. IRC energy profile of the deprotonation of I2. Distances are given in [A]. Inset graph shows a close-up of the region where proton passes to DMF.

changes because the proton is first transferred to one of the DMF molecules, and afterward, these molecules adjust their position and the proton becomes trapped between two DMF's. Therefore, the pair of DMF molecules, with the two carbonyl groups, works like a pair of pliers, extracting the proton from the intermediate and enabling the further progress of the reaction. At the transition state (TS2), the contacts between atoms involved in the proton transfer are very close; i.e., the N1−H distance is 2.07, and the O−H distances are 1.0 (first DMF molecule) and 2.02 Å (second DMF molecule). The four atoms involved are almost in plane, with hydrogen in the middle and oxygen and nitrogen separated by angles 102, 128, and 131°. The changes in the charge distribution can be monitored by looking at the point charges (Table 5). When bound to the imidazole ring, the hydrogen has positive charge of 0.32e; after dissociation and trapping between DMF molecules, it becomes more positive (0.50e). Accordingly, the negative charge is recovered in the imidazole ring; N1 and C4 become more negative (from −0.09e to −0.30e and from 0.13e to −0.03e, respectively). When the hydrogen binds to the DMF molecule, the oxygen atom of the latter becomes less negative (from −0.61e to −0.56e). At the same time, the point charges at the second DMF molecule change; the oxygen charge drops from −0.56e to −0.64e, but the C center becomes more positive (from 0.39e to 0.47e) and the N center−more negative (from 0.06e to −0.10e).

Second Substitution at N1. The second substitution (I3 → P), similarly to the first, can proceed either according to the S_N2 mechanism, with direct substitution of the chloromethyl ether at the N1 center, or via a cation stabilized by a DMF molecule. The energy barrier for the direct transfer is 7.4 kcal/mol at the X3LYP level of theory and 13.6 kcal/mol at MP2//X3LYP, slightly higher than for the first step, which is probably due to the local configuration of the molecules. The barrier for the transfer to DMF is 8.5 kcal/mol (X3LYP) or 12.8 kcal/mol. The barrier for the subsequent transfer from DMF to

dx.doi.org/10.1021/jo502317m | J. Org. Chem. 2015, 80, 237−246

Table 5. CHELPG Charges at Selected Centers of the Species Involved in the Second and Third Steps of the Reaction. Charges Computed at X3LYP/6-31+G(d)//MP2/6-31+G(d) Level of Theory

	step 2											
	imidazole ring						DMF molecule 1			DMF molecule 2		
	N1	H1	C2H[a]	N3	C4H[a]	C5H[a]	O	C1	N	O	C1	N
I2	−0.090	0.325	0.209	−0.082	0.132	0.068	−0.611	0.467	−0.101	−0.565	0.394	0.064
TS2	−0.274	0.379	0.150	0.004	0.007	0.047	−0.534	0.544	0.026	−0.529	0.364	−0.044
I3	−0.303	0.500	0.162	−0.090	−0.032	0.106	−0.562	0.489	0.065	−0.643	0.467	−0.099
	step 3											
	imidazole					ether			DMF			
	N1	C2H[a]	N3	C4H[a]	C5H[a]	CL	C1H$_2$[a]	O	O	C1H[a]	N	
I3	−0.303	0.162	−0.090	−0.032	0.106	−0.201	0.304	−0.255	−0.532	0.308	−0.063	
TS3	−0.325	0.170	−0.127	0.001	0.075	−0.839	0.654	−0.303				
P	−0.067[c]	0.244	[c]	0.051[d]	[d]	−0.957	0.427	−0.444	−0.431	0.349	−0.068	
	0.024[c]			0.068[d]		−0.955[b]	0.470[b]	−0.465[b]				
TS3a	−0.331	0.234	−0.118	0.005	0.076	−0.903	0.693	−0.355	−0.551	0.425	−0.072	
I3a	−0.365	0.211	−0.075	−0.009	0.080	−0.969	0.535	−0.476	−0.322	0.477	0.000	
TS3b	−0.284	0.184	−0.105	0.026	0.056	−0.956	0.549	−0.245	−0.497	0.480	−0.097	

[a]Hydrogen atom charges added to heavy atom. [b]Charges on the second/third DMF molecule. [c]N1 is equivalent to N3. [d]C4 is equivalent to C5.

methoxymethyl-substituted imidazole is 8.4 kcal at the X3LYP level and 11.8 kcal/mol at the MP2//X3LYP level (calculated with respect to I3 intermediate). Therefore, like for the first step of the reaction the direct and DMF-mediated routes seem competitive, but due to the abundance of DMF, the mediated pathway should be more likely. Also the analysis of distances and angles shows (Figure 5) that the first and third step are similar. Substitution of the chloromethyl ether leads to the reduction of the negative charge on the imidazole ring; in I3 the nitrogen I3 has charge −0.30e, which becomes −0.07e in P. Also N1 and N3 become equivalent and the latter atom has charge 0.02e. On the other hand, the C1−O bond in ether becomes more polarized—from +0.30/−0.25e in I3 to +0.43/−0.44e in one substituent and +0.47/−0.46e in the other one.

CONCLUSIONS

A new terpene derivative was prepared from the natural chiral pool of (1*R*,2*S*,5*R*)-(−)-menthol with high efficiency. This chiral imidazole derivative, 1-(1*R*,2*S*,5*R*)-(−)-menthoxymethyl-imidazole, is an excellent substrate for quaternization. Furthermore, the symmetrical chiral imidazolium chloride was synthesized using two methods. In the first method, 1,3-bis[(1*R*,2*S*,5*R*)-(−)-menthoxymethyl]imidazolium chloride was prepared by the Menschutkin reaction using the above mentioned 1-(1*R*,2*S*,5*R*)-(−)-(menthoxymethyl)imidazole and chloromethyl (1*R*,2*S*,5*R*)-(−)-menthyl ether as reactants and hexane as a solvent. In the second method, the imidazolium chloride with two (1*R*,2*S*,5*R*)-(−)-menthoxymethyl substituents was synthesized using imidazole and chloromethyl (1*R*,2*S*,5*R*)-(−)-menthyl ether as reactants (S_N2) and DMF as a solvent.

Quantum chemical calculations at the DFT level have been used in order to validate the hypothesis that the symmetric substitution of the chloromethyl (1*R*,2*S*,5*R*)-(−)-menthyl ether to imidazole in DMF proceeds in a three-step reaction where the first substitution is at N3, the second one is at N1, and the latter reaction must be preceded by a proton transfer to a DMF pair. We have shown that the two substitution reactions may progress according to the S_N2 mechanism, when direct transfer is considered, or in two consecutive steps that can be viewed as an S_N1 mechanism. Both routes have activation barriers accessible in ambient conditions. The proton can be indeed removed by a DMF pair, and due to the character of this solvent such a process is not possible in other media. Following the previous hypothesis of Pernak et al.,[30] we postulate that the proton is trapped between the carbonyl groups of DMF molecules, and this is also supported by spectroscopic findings.[33] This ability to stabilize free proton renders DMF different from other solvents used and enables the further progress of the reaction. On the basis of this observation, one can stipulate that a suitable solvent for a one-step synthesis of symmetric imidazolium salts described in this paper would be a polar aprotic solvent that is also a strong Lewis base.

In general 1,3-bis[(1*R*,2*S*,5*R*)-(−)-menthoxymethyl]-imidazolium chloride obtained in those two different procedures is very interesting for a couple of reasons, and its main use is as a synthetic precursor of chiral symmetrical ionic liquids.

However, there is also another aspect, the biological one: chiral imidazolium salts obtained directly from (1*R*,2*S*,5*R*)-(−)-menthol, 3-alkyl-1-[(1*R*,2*S*,5*R*)-(−)-menthoxymethyl]-imidazolium[28] and 3-alkoxymethyl-1-[(1*R*,2*S*,5*R*)-(−)-menthoxymethyl]imidazolium,[29] were described and tested previously. Synthesized chiral chlorides were verified for antimicrobial activity against rods, cocci, bacillus, and fungi.[35] Most of the tested alkylimidazolium and alkoxymethylimidazolium chlorides exhibited activities higher than the ones shown by commonly used pattern (benzalkonium chloride). Noteworthy is the fact that including (1*R*,2*S*,5*R*)-(−)-menthol in the chloride's structure enhances the biological activity of chlorides. Therefore, symmetrical chiral imidazolium chloride currently is being designed and synthesized in our group in order to fully investigate its biological applications. We expect again a broad spectrum of activity against microbes, especially due to the known importance of the (1*R*,2*S*,5*R*)-(−)-menthol moiety.

EXPERIMENTAL SECTION

General Methods. ^{1}H and ^{13}C and NMR spectra were recorded with tetramethylsilane as the standard (at 300 and 75 MHz, respectively). Two-dimensional spectra were performed using standard pulse sequences at 600 MHz. HRMS analysis was performed on mode ESI+ (TOF MS ES+). The spectra are included in the Supporting

dx.doi.org/10.1021/jo502317m | J. Org. Chem. 2015, 80, 237−246

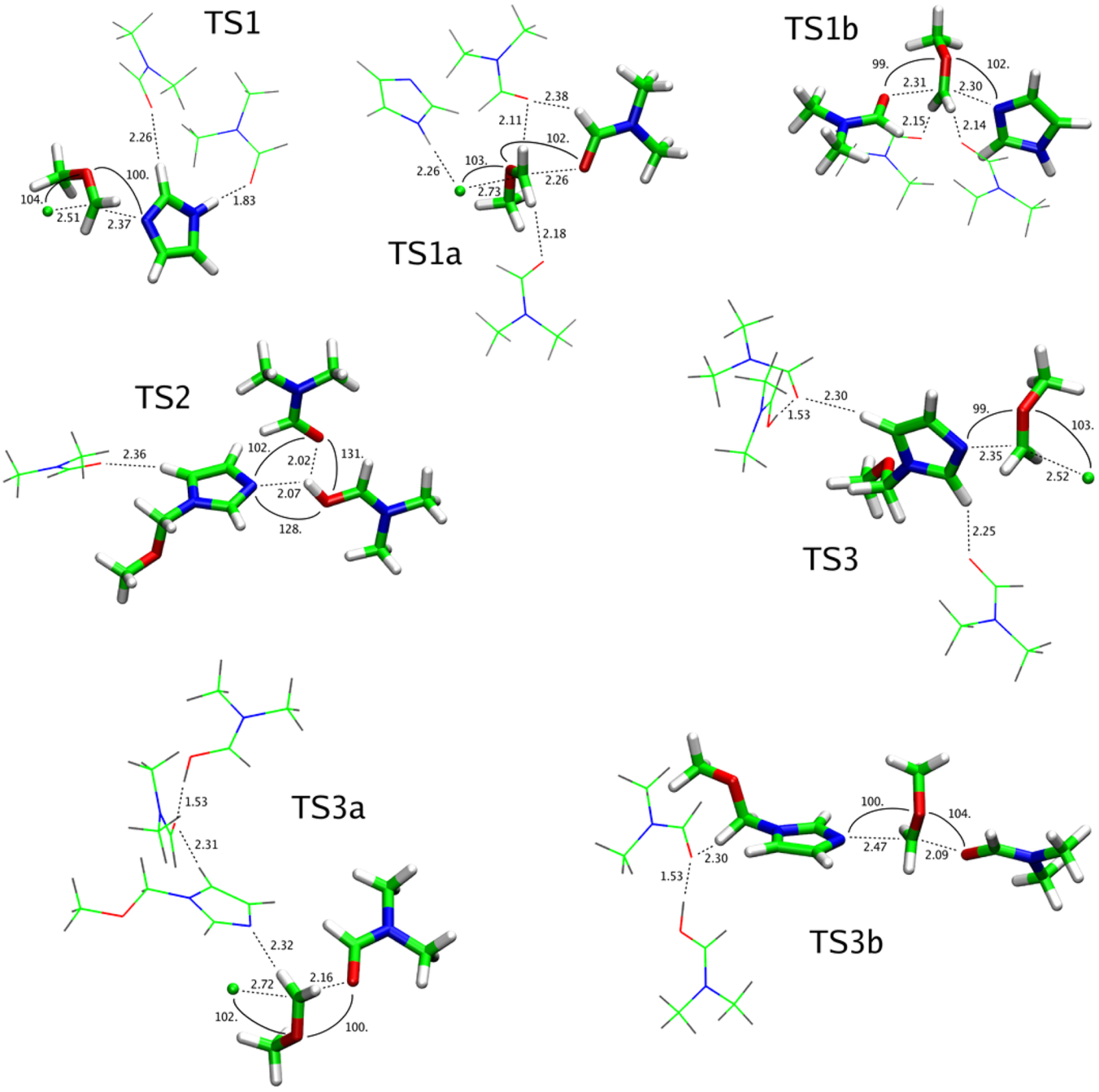

Figure 5. Structures of the TS complexes along the reaction path. Distances are given in angstroms and angles in degrees. Molecules directly involved in a particular step are shown using thick tubes; molecules that do not participate are shown as thin lines or omitted for better clarity.

Information. Melting points were determined by using an electrothermal digital-melting-point apparatus. Optical rotations were measured at 578 nm.

Syntheses. Chloromethyl (1*R*,2*S*,5*R*)-(−)-menthyl ether was prepared by passing HCl through a mixture of paraformaldehyde and (1*R*,2*S*,5*R*)-(−)-menthol.[26] Imidazole was freshly recrystallized from benzene (mp 90−91 °C). Triethylamine was distilled twice, the first time being from phthalic anhydride (this serves to remove lower amines that result from autoxidation during storage).

1-(1R,2S,5R)-(−)-Menthoxymethylimidazole (1). Chloromethyl (1*R*,2*S*,5*R*)-(−)-menthyl ether (10.225 g, 0.05 mol) was slowly added to a stirred anhydrous solution of triethylamine (5.05 g, 0.05 mol) in toluene (50 mL), and stirring was continued at 80 °C for 20 min. Imidazole (3.4 g, 0.05 mol) was then added, and the mixture was refluxed next 30 min. After being cooled to room temperature, the triethylamine hydrochloride produced was filtered off. The organic phase was washed with saturated sodium chloride solution, dried over (Na_2SO_4), and concentrated by rotoevaporation. The product was purified by vacuum distillation. After solidification of the pure, colorless liquids, the white solid was crystallized. The crystalline final product was further dried in vacuum (0.3 mmHg) to afford analytically pure **1** (yield: 98%, 0.049 mol, 11.58 g). ^{1}H NMR (300 MHz, $CDCl_3$): δ 0.45 (d, J = 6.9 Hz, 3H, H9 or H10), 0.80−0.95 (m, 9H, Ha-4, H7, H9 or H10, Ha-6 and Ha-3), 1.15−1.40 (m, 2H, H2 and H5), 1.58−1.65 (m, 2H, Hb-3 and Hb-4), 1.87−1.95 (m, 1H, Hb-6), 2.01 (sept d, J = 7.1 Hz and J = 2.6, 1H, H8), 3.12 (td, J = 10.6 Hz and J = 4.3 Hz, 1H, H1), 5.32 (m, 2H, H11), 7.04−7.05 (m, 1H, H13), 7.08 (m, 1H, H12), 7.59 (m, J = 1.1 Hz, 1H, H14). ^{13}C NMR (300 MHz, $CDCl_3$): δ 15.0 (C9 or C10), 20.5 (C7), 21.7 (C9 or C10), 22.5 (C3), 24.8 (C8), 30.8 (C5), 33.7 (C4), 39.5 (C6), 47.4 (C2), 73.2 (C1), 76.5 (C11),

dx.doi.org/10.1021/jo502317m | J. Org. Chem. 2015, 80, 237−246

118.5 (C13), 129.2 (C12), 136.8 (C14). HRMS (ESI +) m/z calcd for $[C_{14}H_{24}N_2O]^+$ 237.1967, found 237.1978. Anal. Calcd for $C_{14}H_{24}N_2O$: C, 71.12; H, 10.25; N, 11.85. Found: C, 70.96; H, 10.51; N, 11.73.

*1,3-Bis[(1R,2S,5R)-(−)-menthoxymethyl]imidazolium Chloride (**2**). Method I.* Chloromethyl (1*R*,2*S*,5*R*)-(−)-menthyl ether (6.135 g, 0.03 mol) was added dropwise into a round-bottomed flask which contained a vigorously stirred mixture of 30 mL of dry hexane and crystallized 1-(1*R*,2*S*,5*R*)-(−)-(menthoxymethyl)imidazole (7.09 g, 0.03 mol). The reaction mixture was stirred at room temperature for 45 min. After 120 min, the phases were separated, and the crude product was washed with dry hexane (3 × 30 mL). The volatile materials were removed under reduced pressure (0.3 mmHg) at 60 °C overnight. The obtained white solid was recrystallized and further dried in vacuum (0.3 mmHg) to afford analytically pure **2** (yield: 93%, 0.028 mol, 12.31 g). ^{1}H NMR (2D NMR, 600 MHz, $CDCl_3$): δ 0.55 (d, J = 6.9 Hz, 6H, H9 or H10 and H9′ or H10′), 0.79−0.95 (m, 18H, Ha-4, H7, H9 or H10, Ha-6, Ha-3, Ha-4′, H7′, H9′ or H10′, Ha-6′ and Ha-3′), 1.22−1.29 (m, 2H, H2 and H2′), 1.42−1.45 (m, 2H, H5 and H5′), 1.58−1.66 (m, 4H, Hb-3, Hb-4, Hb-3′ and Hb-4′), 1.98 (sept d, J = 6.9 Hz, J = 2.5 Hz, 2H, H8 and H8′), 2.11 (d, J = 11.9 Hz, 2H, Hb-6 and Hb-6′), 3.39 (td, J = 10.5 Hz, J = 4.2 Hz, 2H, H1 and H1′), 5.68 and 5.92 (d, J = 10.5 Hz, 4H, AB system, H11 and H11′), 7.48 (m, 1H, H12 and H13), 11.38 (m, 1H, H14). ^{13}C NMR (300 MHz, $CDCl_3$): δ 15.6 (C9 or C10 and C9′ or C10′), 20.8 (C7 and C7′), 22.0 (C9 or C10 and C9′ or C10′), 22.6 (C3 and C3′), 25.3 (C8 and C8′), 31.0 (C5 and C5′), 33.8 (C4 and C4′), 40.2 (C6 and C6′), 47.6 (C2 and C2′), 77.1 (C1 and C1′), 80.0 (C11 and C11′), 121.1 (C13 and C12), 137.7 (C14). Anal. Calcd for $C_{25}H_{45}ClN_2O_2$: C, 68.06; H, 10.30; N, 6.35. Found: C, 67.82; H, 10.39; N, 6.46.

Method II. Chloromethyl (1*R*,2*S*,5*R*)-(−)-menthyl ether (6.135 g, 0.03 mol, 2 equiv) was added dropwise into a round-bottomed flask which contained a stirred mixture of 35 mL of dry DMF and imidazole (1.02 g, 0.015 mol, 1 equiv). The solution was stirred at 35 °C for 2 h and then cooled to room temperature. Then DMF was expelled from the reaction mixture under reduced pressure, and the product was washed with warm, dry hexane (3 × 30 mL). The volatile materials were removed under reduced pressure (0.3 mmHg) at 60 °C overnight. The crude product was obtained as a light yellow solid. After crystallization, the final product was further dried in vacuum (0.3 mmHg) to afford analytically pure **2** (yield: 83.5%, 0.0125 mol, 5.52 g).The material was identical (^{1}H and ^{13}C NMR) with material prepared previously by method I.

Quantum Chemical Calculations of the Reaction in DMF. The reactions involved in the one-step synthesis have been modeled by quantum chemical calculations. The full model of the reacting system, including two molecules of chloromethyl (1*R*,2*S*,5*R*)-(−)-menthyl ether, imidazole, and solvent molecules is beyond the capabilities of the present high-level quantum chemical calculations due to its size (up to 113 atoms). On the other hand, the menthyl substituent can be hardly expected to have other than sterical effects. Therefore, the (1*R*,2*S*,5*R*)-(−)-menthoxymethyl component has been replaced with a methoxy group (forming chloromethylmethyl ether, $ClCH_2OCH_3$), reducing the size of the model to 63 atoms. Another justification of this simplification is the fact that a similar mechanism has been observed when alkyl chloromethyl ethers are used.[30] The reaction was characterized by finding minima (reactant-, product- and intermediate states) and saddle points (transition states, TS) on the potential energy hypersurface. In order to calculate the reaction energies and barriers, van der Waals complexes of reactants/products were used, rather than isolated species, which would introduce basis set superposition errors (BSSE). Initial tests have been done for an isolated model, with no, one, or two solvent molecules explicitly included and with a polarizable continuum model (PCM) in order to simulate the specific interactions with the solvent as well as its long-range influence. It has been shown that this model is an economic and reliable way to introduce long-range solvation effects.[37,38] The PCM model assumed relative permittivity of 37.2, corresponding to DMF.[39] In the course of calculations, various models have been employed: for the first step, we have used six different models to study how the solvent affects the reaction kinetics and thermodynamics; these models are Ini-0, Ini-1, Ini-2, Ini-0/PCM, Ini-1/PCM, and Ini-2/PCM. The final production model used for all steps of the reaction included one imidazole molecule, two chloromethyl ether molecules, and three DMF molecules. The chemical composition of the models is shown in the Table SI-1 (Supporting Information). All models have been optimized at the density functional theory (DFT) level using hybrid X3LYP functional[36] and a GTO basis set 6-31+G(d). Diffuse functions have been added due to the presence of negatively charged chloride anion. For the sake of simplicity, this level of theory (X3LYP/6-31+G(d)) is referred to as X3LYP. All minima and saddle points have been confirmed by computing the Hessian matrix. Saddle points (TSs) were required to have exactly one imaginary frequency, while minima were required to have no imaginary frequencies. Additionally, the intrinsic reaction coordinate (IRC) method using the local quadratic approximation[39,40] was used to step "downhill" from the TS2 (step 2) in both directions (i.e., toward both intermediates). The energy of each state found was recalculated at the Møller−Plesset 2 (MP2) level of theory using the same basis set, in order to verify the approximate model of electron correlation used by DFT. Atomic point charges have also been calculated at the MP2/6-31+G(d) level of theory by fitting the electrostatic potential at CHELPG mesh of points. This level of theory will be further referred to as MP2. Next, the zero-point and thermal corrections to the energy have been computed at X3LYP/6-the 31+G(d) level, assuming a temperature of 298 K, pressure of 1 atm, and the rigid rotator/harmonic oscillator models. On the basis of these corrections, Gibbs free energy was estimated. All calculations have been done in the Gaussian 2009 package.[41]

X-ray Structure Determination. X-ray diffraction data were collected at 100(1) K by the ω-scan technique on a four-circle diffractometer equipped with a detector[42] equipped with Mo Kα radiation source (λ = 0.71073 Å). The data were corrected for Lorentz polarization effects as well as for absorption (multiscan).[42] Accurate unit-cell parameters were determined by a least-squares fit of and 2180 reflections of highest intensity, chosen from the whole experiment. The calculations were mainly performed within the WinGX program system.[43] The structures were solved with SIR92[44] and refined with the full-matrix least-squares procedure on F^2 by SHELXL97.[45] Scattering factors incorporated in SHELXL97 were used. The function $\Sigma w(|F_o|^2 - |F_c|^2)^2$ was minimized, with $w^{-1} = [\sigma^2(F_o)^2 + (0.065P)^2]$, where $P = [\max(F_o^2, 0) + 2F_c^2]/3$. All non-hydrogen atoms were refined anisotropically, and all hydrogen atoms were placed geometrically, in idealized positions, and refined as riding group with their U_{iso}'s set at 1.2 (1.5 for methyl groups) × U_{eq} of appropriate carrier atom.

Crystal data: $C_{14}H_{24}N_2O$, M_r = 236,35, monoclinic, space group $P2_1$, a = 6.2999(11) Å, b = 7.7215912) Å, c = 14.823(2) Å, β = 95.614(13)°, V = 717.6(2) Å^3, Z = 2, d_x = 1.09 g·cm^{-3}, $F(000)$ = 260, μ(Mo Kα) = 0.069 mm^{-1}. 4678 reflections collected up to 2Θ = 52°, 2219 symmetry-independent (R_{int} = 0.029), 2020 with $I > 2\sigma(I)$. Final $R(F)$ = 4.74% ($I > 2\sigma(I)$), 5.21% (all reflections), w$R(F^2)$ = 0.119 ($I > 2\sigma(I)$), 0.123 (all reflections), S = 1.10. In the final residual map, $\Delta\rho_{max}/\Delta\rho_{min}$ = 0.27/−0.28 e·Å^{-3}.

■ ASSOCIATED CONTENT

Supporting Information

All spectroscopic data for all compounds. Hydrogen bond data and crystal structure of compound **1**. Cartesian coordinates of stationary points and transition state, as well as the coordinates of IRC points for step 2; movie clip of the proton transfer in step 2, based on the IRC path. All relevant crystallographic information (CIF). This material is available free of charge via the Internet at http://pubs.acs.org. Crystallographic data (excluding structure factors) for the structural analysis has been deposited with the Cambridge Crystallographic Data Centre. Additionally, data for room temperature structures have been also deposited as CCDC 1027600. Copies of this information may be obtained free of charge from the Director, CCDC, 12 Union Road, Cambridge, CB2 1EZ, UK. Fax:

dx.doi.org/10.1021/jo502317m | J. Org. Chem. 2015, 80, 237−246

+44(1223)336-033, e-mail: deposit@ccdc.cam.ac.uk, or www.ccdc.cam.ac.uk.

AUTHOR INFORMATION

Corresponding Author

*E-mail: joanna.feder-kubis@pwr.edu.pl.

Notes

The authors declare no competing financial interest.

ACKNOWLEDGMENTS

This research was financed by the National Science Centre (Poland) (Grant No. 2011/01/B/ST5/06659). Calculations have been carried out at the Wroclaw Centre for Networking and Supercomputing (http://www.wcss.wroc.pl).

REFERENCES

(1) Seddon, K. R. *J. Chem. Technol. Biotechnol.* **1997**, *68*, 351−356.
(2) Larsen, A. S.; Holbrey, J. D.; Tham, F. S.; Reed, C. A. *J. Am. Chem. Soc.* **2000**, *122*, 7264−7272.
(3) Binnemans, K. *Chem. Rev.* **2005**, *105*, 4148−4204.
(4) Yang, M.; Mallick, B.; Mudring, A.-V. *Cryst. Growth Des.* **2013**, *13*, 3068−3077.
(5) Rogers, R. D.; Seddon, K. R. *Science* **2003**, *302*, 792−793.
(6) Lee, K. M.; Lee, C. K.; Lin, I. J. B. *Chem. Commun.* **1997**, 899−900.
(7) Gordon, C. M.; Holbrey, J. D.; Kennedy, A. R.; Seddon, K. R. *J. Mater. Chem.* **1998**, *8*, 2627−2636.
(8) Dzyuba, S. V.; Bartsch, R. A. *Chem. Commun.* **2001**, 1466−1467.
(9) Wang, X. J.; Heinemann, F. W.; Yang, M.; Mechler, B. U.; Fekete, M.; Mudring, A.-V.; Wasserscheid, P.; Meyer, K. *Chem. Commun.* **2009**, 7405−7407.
(10) Anderson, J. L.; Ding, R.; Ellern, A.; Armstrong, D. W. *J. Am. Chem. Soc.* **2005**, *127*, 593−604.
(11) Zheng, W.; Mohammed, A.; Hines, L. G., Jr.; Xiao, D.; Martinez, O. J.; Bartsch, R. A.; Simon, S. L.; Russina, O.; Triolo, A.; Quitevis, E. L. *J. Phys. Chem. B* **2011**, *115*, 6572−6584.
(12) Yoshida, Y.; Saito, G. *Phys. Chem. Chem. Phys.* **2011**, *13*, 20302−20310.
(13) Pernak, J.; Skrzypczak, A.; Lota, G.; Frackowiak, E. *Chem.—Eur. J.* **2007**, *13*, 3106−3112.
(14) Chang, J.-C.; Ho, W.-Y.; Sun, I.-W.; Chou, Y.-K.; Hsieh, H.-H.; Wua, T.-Y. *Polyhedron* **2011**, *30*, 497−507.
(15) Payagala, T.; Huang, J.; Breitbach, Z. S.; Sharma, P. S.; Armstrong, D. W. *Chem. Mater.* **2007**, *19*, 5848−5850.
(16) Jin, C.-M.; Ye, C.; Phillips, B. S.; Zabinski, J. S.; Liu, X.; Liu, W.; Shreeve, J. M. *J. Mater. Chem.* **2006**, *16*, 1529−1535.
(17) Han, X.; Armstrong, D. W. *Org. Lett.* **2005**, *7*, 4205−4208.
(18) Xiao, J.-C.; Shreeve, J. M. *J. Org. Chem.* **2005**, *70*, 3072−3078.
(19) Wang, R.; Jin, C.-M.; Twamley, B.; Shreeve, J. M. *Inorg. Chem.* **2006**, *45*, 6396−6403.
(20) Anderson, J. L.; Armstrong, D. W.; Wei, G.-T. *Anal. Chem.* **2006**, *78*, 2893−2902.
(21) Lambertus, G. R.; Crank, J. A.; McGuigan, M. E.; Kendler, S.; Armstrong, D. W.; Sacks, R. D. *J. Chromatogr. A* **2006**, *1135*, 230−240.
(22) Carda-Broch, S.; Berthod, A.; Armstrong, D. W. *Rapid Commun. Mass Spec.* **2003**, *17*, 553−560.
(23) Soukup-Hein, R. J.; Remsburg, J. W.; Dasgupta, P. K.; Armstrong, D. W. *Anal. Chem.* **2007**, *79*, 7346−7352.
(24) Yua, G.; Yana, S.; Zhoub, F.; Liub, X.; Liub, W.; Lianga, Y. *Tribol. Lett.* **2007**, *25*, 197−205.
(25) Messali, M.; Moussa, Z.; Alzahrani, A. Y.; El-Naggar, M. Y.; ElDouhaibi, A. S.; Judeh, Z. M. A.; Hammouti, B. *Chemosphere* **2013**, *91*, 1627−1634.
(26) Pernak, J.; Feder-Kubis, J. *Chem.—Eur. J.* **2005**, *11*, 4441−4449.
(27) Pernak, J.; Feder-Kubis, J. *Tetrahedron: Asymmetry* **2006**, *17*, 1728−1737.
(28) Pernak, J.; Feder-Kubis, J.; Cieniecka-Rosłonkiewicz, A.; Fischmeister, C.; Griffin, S.; Rogers, R. *New J. Chem.* **2007**, *31*, 879−892.
(29) Feder-Kubis, J.; Kubicki, M.; Pernak, J. *Tetrahedron: Asymmetry* **2010**, *21*, 2709−2718.
(30) Pernak, J.; Sobaszkiewicz, K.; Foksowicz-Flaczyk, J. *Chem.—Eur. J.* **2004**, *10*, 3479−3485.
(31) Holbrey, J. D.; Rogers, R. D. *Ionic Liquids in Synthesis*, 2nd. ed.; Welton, T.; Wasserscheid, P., Eds.; Wiley-VCH: Weinheim, 2008; Vol. *1*, p 66.
(32) Huang, Z.; Yu, L.; Dai, Y.; Wang, H. *Struct. Chem.* **2011**, *22*, 57−65.
(33) Dimitriev, O. P.; Kislyuk, V. V. *J. Phys. Chem. A* **2005**, *109*, 2459−2464.
(34) Dimitriev, O. P.; Kislyuk, V. V. *Spectrochim. Acta Part A* **2007**, *68*, 29−35.
(35) Feder-Kubis, J.; Tomczuk, K. *Tetrahedron* **2013**, *69*, 4190−4198.
(36) Xu, X.; Goddard, W. A., III. *Proc. Natl. Acad. Sci. U.S.A.* **2004**, *101*, 2673−2677.
(37) Cossi, M.; Barone, V.; Cammi, R.; Tomasi, J. *Chem. Phys. Lett.* **1996**, *255*, 327−335.
(38) Mennucci, B.; Tomasi, J. *J. Chem. Phys.* **1997**, *106*, 5151−5158.
(39) Page, M.; McIver, J. W., Jr. *J. Chem. Phys.* **1988**, *88*, 922−935.
(40) Page, M.; Doubleday, C., Jr.; McIver, J. W., Jr. *J. Chem. Phys.* **1990**, *93*, 5634−5642.
(41) Frisch, M. J.; Trucks, G. W.; Schlegel, H. B.; Scuseria, G. E.; Robb, M. A.; Cheeseman, J. R.; Scalmani, G.; Barone, V.; Mennucci, B.; Petersson, G. A.; Nakatsuji, H.; Caricato, M.; Li, X.; Hratchian, H. P.; Izmaylov, A. F.; Bloino, J.; Zheng, G.; Sonnenberg, J. L.; Hada, M.; Ehara, M.; Toyota, K.; Fukuda, R.; Hasegawa, J.; Ishida, M.; Nakajima, T.; Honda, Y.; Kitao, O.; Nakai, H.; Vreven, T.; Montgomery, J. A., Jr.; Peralta, J. E.; Ogliaro, F.; Bearpark, M.; Heyd, J. J.; Brothers, E.; Kudin, K. N.; Staroverov, V. N.; Keith, T.; Kobayashi, R.; Normand, J.; Raghavachari, K.; Rendell, A.; Burant, J. C.; Iyengar, S. S.; Tomasi, J.; Cossi, M.; Rega, N.; Millam, J. M.; Klene, M.; Knox, J. E.; Cross, J. B.; Bakken, V.; Adamo, C.; Jaramillo, J.; Gomperts, R.; Stratmann, R. E.; Yazyev, O.; Austin, A. J.; Cammi, R.; Pomelli, C.; Ochterski, J. W.; Martin, R. L.; Morokuma, K.; Zakrzewski, V. G.; Voth, G. A.; Salvador, P.; Dannenberg, J. J.; Dapprich, S.; Daniels, A. D.; Farkas, O.; Foresman, J. B.; Ortiz, J. V.; Cioslowski, J.; Fox, D. J. *Gaussian 09, Revision B.01*, Gaussian, Inc., Wallingford, CT, 2010.
(42) Agilent Technologies, 2010. CrysAlis^{PRO}.
(43) Farrugia, L. J. *J. Appl. Crystallogr.* **1999**, *32*, 837−838.
(44) Altomare, A.; Cascarano, G.; Giacovazzo, C.; Guagliardi, A. *J. Appl. Crystallogr.* **1993**, *26*, 343−350.
(45) Sheldrick, G. M. *Acta Crystallogr.* **2008**, *A64*, 112−122.